Supplement of Atmos. Chem. Phys., 20, 13701–13719, 2020
https://doi.org/10.5194/acp-20-13701-2020-supplement

*Supplement of*

# Photooxidation of pinonaldehyde at ambient conditions investigated in the atmospheric simulation chamber SAPHIR

**Michael Rolletter et al.**

*Correspondence to:* Hendrik Fuchs (h.fuchs@fz-juelich.de)

## Supplement

### Model modifications based on Fantechi et al. (2002)

All additions and modifications made in the sensitivity runs Fantechi_a and Fantechi_b based on the suggestions by Fantechi et al. (2002) are shown in Table S1. The naming schema of reactants starting with an “R” is according to Fantechi et al. (2002).

In our calculations the exclusive fate of FAN_C3 is the formation of 4-hydroxynorpinonaldehyde and $\mathrm{HO_2}$. Fantechi et al. (2002) state that at high NO conditions used in laboratory experiments, formic acid (HCOOH) could be formed instead.

To account for possible $\mathrm{RO_2 + HO_2}$ reactions, a reaction scheme based on the reaction $\mathrm{C97O2 + HO_2}$ is added for all newly introduced $\mathrm{RO_2}$ species not included in the MCM. $\mathrm{RO_2}$ form a corresponding hydroxyperoxide (ROOH) that can either react with OH to regenerate the $\mathrm{RO_2}$ or photolyse to form the corresponding alkoxy radical (RO) that would be also formed by the reaction of $\mathrm{RO_2 + NO}$. The general scheme is shown here for one $\mathrm{RO_2}$ as an example:

$$\mathrm{FAN\_C1 + HO_2} \rightarrow \mathrm{FAN\_C1\_HO2} \quad \mathrm{(KRO2HO2)} \tag{R-S1}$$

$$\mathrm{FAN\_C1\_HO2 + OH} \rightarrow \mathrm{FAN\_C1} \quad (1 \times 10^{-11}\mathrm{cm^3 s^{-1}}) \tag{R-S2}$$

$$\mathrm{FAN\_C1\_HO2} + \mathrm{h}\nu \rightarrow \mathrm{R\_O3} \quad (\mathrm{J_{22}}) \tag{R-S3}$$

$$\mathrm{FAN\_C1\_HO2} + \mathrm{h}\nu \rightarrow \mathrm{R\_O3} \quad (\mathrm{J_{41}}) \tag{R-S4}$$

Reaction rate constants were used as stated in the MCM.

**Table S1.** Additional and modified reactions applied to the MCM based on the proposed mechanism by Fantechi et al. (2002). Names are taken from the MCM where existing. Newly introduced species are named either with the prefix “FAN” or “R”. All nitrate species are lumped as one species RNO3.

| reaction | reaction rate constant |
|---|---|
| PINAL + OH → C96CO3 | $0.61 \times 5.2 \times 10^{-12} \exp(600\mathrm{K}/\mathrm{T})\,\mathrm{cm}^3\mathrm{s}^{-1}$ |
| PINAL + OH → FAN_D1 | $0.24 \times 5.2 \times 10^{-12} \exp(600\mathrm{K}/\mathrm{T})\,\mathrm{cm}^3\mathrm{s}^{-1}$ |
| PINAL + OH → PINALO2 | $0.09 \times 5.2 \times 10^{-12} \exp(600\mathrm{K}/\mathrm{T})\,\mathrm{cm}^3\mathrm{s}^{-1}$ |
| PINAL + OH → FAN_G1 | $0.06 \times 5.2 \times 10^{-12} \exp(600\mathrm{K}/\mathrm{T})\,\mathrm{cm}^3\mathrm{s}^{-1}$ |
| C96O → NORPINAL + $HO_2$ | $5.0 \times 10^4\,\mathrm{s}^{-1}$ |
| C96O → FAN_C1 | $6.5 \times 10^5\,\mathrm{s}^{-1}$ |
| FAN_C1 + NO → R_O3 + $NO_2$ | 0.86× KRO2NO[a] |
| FAN_C1 + NO → RNO3 | 0.14× KRO2NO[a] |
| R_O3 → FAN_C2 + HCHO | $1.2 \times 10^7\,\mathrm{s}^{-1}$ |
| R_O3 → FAN_C3 | $3.2 \times 10^8\,\mathrm{s}^{-1}$ |
| FAN_C2 + NO → R_O5 +$NO_2$ | 0.91× KRO2NO[a] |
| FAN_C2 + NO → RNO3 | 0.09× KRO2NO[a] |
| FAN_C3 → NORPINALOH + $HO_2$ | $2.0 \times 10^3\,\mathrm{s}^{-1}$ |
| R_O5 → FAN_C5 | 0.5× KDEC[b] |
| R_O5 → FAN_C6 | 0.5× KDEC[b] |
| FAN_C5 + NO → FAN_C7 + $NO_2$ | 0.75× KRO2NO[a] |
| FAN_C5 + NO → RNO3 | 0.25× KRO2NO[a] |
| FAN_C6 + NO → HCHO + $HO_2$ + $NO_2$ | 0.93× KRO2NO[a] |
| FAN_C6 + NO → RNO3 | 0.07× KRO2NO[a] |
| FAN_D1 + NO → R_O8 + $NO_2$ | 0.72× KRO2NO[a] |
| FAN_D1 + NO → RNO3 | 0.28× KRO2NO[a] |
| R_O8 → NORPINAL + $HO_2$ | KDEC[b] |
| FAN_G1 + NO → FAN_G2 + $NO_2$ | KRO2NO[a] |
| FAN_G2 + NO → R_O13 + $NO_2$ | 0.89× KRO2NO[a] |
| FAN_G2 + NO → RNO3 | 0.11× KRO2NO[a] |
| R_O13→ FAN_G3 | $5.0 \times 10^{11}\,\mathrm{s}^{-1}$ |
| FAN_G3 + NO → R_O14 + $NO_2$ | KRO2NO[a] |
| R_O14→ FAN_G4 + $CO_2$ | KDEC[b] |
| FAN_G4 + NO → R_O15 + $NO_2$ | 0.86× KRO2NO[a] |
| FAN_G4 + NO → RNO3 | 0.14× KRO2NO[a] |
| R_O15→ FAN_G5 | $0.5 \times 1.0 \times 10^5\,\mathrm{s}^{-1}$ |
| R_O15→ FAN_G7 | $0.5 \times 1.0 \times 10^5\,\mathrm{s}^{-1}$ |
| FAN_G5 + NO → R_O16 + $NO_2$ | 0.97× KRO2NO[a] |
| FAN_G5 + NO → RNO3 | 0.03× KRO2NO[a] |
| R_O16→ C818CO + HCHO + $HO_2$ | KDEC[b] |
| FAN_G7 + NO → R_O17 + $NO_2$ | 0.97× KRO2NO[a] |
| FAN_G7 + NO → RNO3 | 0.03× KRO2NO[a] |
| R_O17→ CO23C4CHO + CH3COCH3 + $HO_2$ | KDEC[b] |

[a] value from MCM: KRO2NO= $2.7 \times 10^{-12} \exp(360\mathrm{K}/\mathrm{T})\,\mathrm{cm}^3\mathrm{s}^{-1}$ (MCM, 2017)

[b] value from MCM: KDEC= $1.0 \times 10^6\,\mathrm{s}^{-1}$ (MCM, 2017)

## Sensitivity study S1 and additional sensitivity tests

In S1 the impact of hypothetical isomerization reactions of all 4 initially formed $RO_2$ radicals on model results was tested. Reactions shown in Tab. S2 were added to the model based on Fantechi et al. (2002). Possible isomerziation reactions in later stages of the mechanism were not tested.

**Table S2.** Overview of added reactions for sensitivity run S1.

| reaction | reaction rate constant |
|---|---|
| C96CO3 $\rightarrow$ $HO_2$ | $0.1\,s^{-1}$ |
| PINALO2 $\rightarrow$ $HO_2$ | $0.1\,s^{-1}$ |
| FAN_D1 $\rightarrow$ $HO_2$ | $0.1\,s^{-1}$ |
| FAN_G1 $\rightarrow$ $HO_2$ | $0.1\,s^{-1}$ |

However, only PINALO2, FAN_D1, and FAN_G1 have an aldehyde group with a hydrogen that can be easily abstracted. An additional sensitivity study (S1_mod) was performed that includes only isomerization reactions of these 3 $RO_2$ applying the same reaction rates used for S1. Figure S1 shows the calculated $HO_2$ and OH time series together with results from S1, model base case (MCM_a), and modified mechanism by Fantechi et al. (2002) (FAN_a).

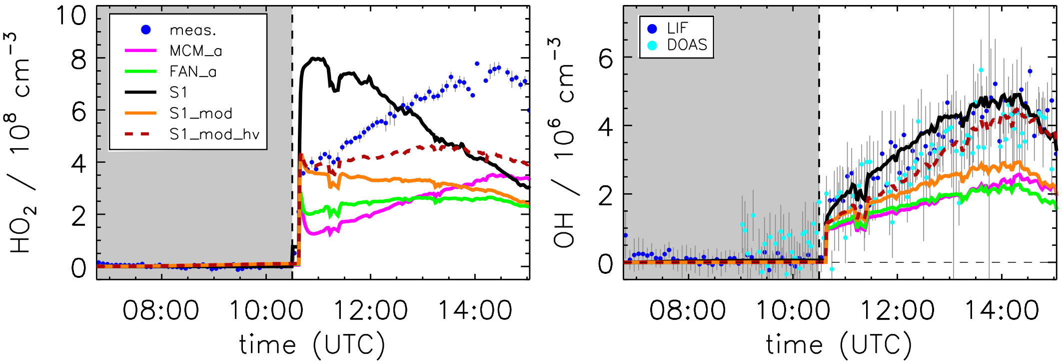

**Figure S1.** Model sensitivity studies of the impact of potential additional $HO_2$ formation by unimolecular $RO_2$ reactions of all 4 initial $RO_2$ (S1) and for $RO_2$ radicals with a –HCO group (S1_mod). The sensitivity test S1_mod_hv extends S1_mod by an additional photolysis of isomerization products. In addition, the model base case (MCM_a) and the case using the mechanism by Fantechi et al. (2002) (FAN_a) are shown. Grey shaded areas indicate times when the chamber roof was closed.

These $RO_2$ radicals are formed with a yield of 39 %. Therefore, $HO_2$ concentrations in the beginning of the experiment are reduced by a factor of 2 compared to S1 where the isomerization of all initial $RO_2$ leads to the formation of $HO_2$. The reduced $HO_2$ concentrations agree with observations at the start of the photooxidation, but show the same temporal trend as in model run S1 over the course of the experiment. This leads to an increasing model-measurement discrepancy of $HO_2$ concentrations of a factor of up to 3. Consistently, OH concentrations are reduced by a factor of 2 compared to S1.

Products of the rapid isomerization reaction could be peroxy acids with additional carbonyl functions. As seen for pinonaldehyde, photolysis frequencies of bi-carbonyl compounds could be generally underestimated in current models. An additional sensitivity test (S1_mod_hv) with isomerization of initially formed $RO_2$ with –HCO group followed by photolysis of the isomerization products with the photolysis frequency of glyoxal was performed. Because the photolysis frequency of glyoxal is slow compared to the reaction rate of the isomerization reaction, the $HO_2$ concentration time series in this sensitivity model run is similar to the sensitivity run with only isomerization (S1_mod). The formation of $HO_2$ is linked to the $RO_2$ concentration in this case and underestimated by the model.

## Sensitivity test of $RO_2 + NO$ reaction rate constants

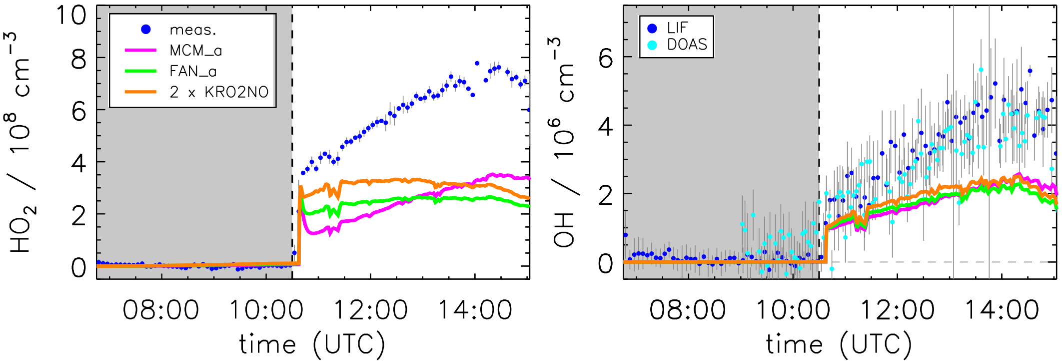

**Figure S2.** Model sensitivity run with modified reaction rate of 2xKRO2NO. The modified reaction rate constant was applied to all $RO_2$ that were introduced by the model modifications based on Fantechi et al. (2002). Grey shaded areas indicate times when the chamber roof was closed.

## Sensitivity study S3

In the used mechanism based on Fantechi et al. (2002) 4-hydroxynorpinonaldehyde was formed as main product with an overall yield of approximately 25 % but no subsequent chemistry was considered in the MCM model and the modified Fantechi mechanism. To investigate if the subsequent chemistry of this product has the potential to partly explain the missing $HO_2$ source a mechanism was deduced from structure–activity relationship (SAR; Kwok and Atkinson, 1995; Vereecken and Peeters, 2009; Vereecken and Nozière, 2020). No theoretical calculations were performed.

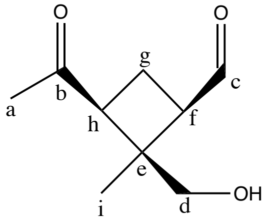

**Figure S3.** Structure of 4-hydroxynorpinonaldehyde and C-atom labeling.

The 4-hydroxynorpinonaldehyde structure is shown in Fig. S3. Reaction rate constants for the H-abstraction by OH were estimated based on Kwok and Atkinson (1995) and are shown in Table S3.

**Table S3.** Reaction rate constants for H-abstraction by OH for different carbon atoms based on Kwok and Atkinson (1995).

| C-atom | reaction rate constant | fraction |
|---|---|---|
| c | $1.69 \times 10^{-11}$ cm$^3$ s$^{-1}$ | 79 % |
| d | $3.27 \times 10^{-12}$ cm$^3$ s$^{-1}$ | 15 % |
| f | $5.43 \times 10^{-13}$ cm$^3$ s$^{-1}$ | 3 % |
| g | $2.62 \times 10^{-13}$ cm$^3$ s$^{-1}$ | 1 % |
| h | $5.43 \times 10^{-13}$ cm$^3$ s$^{-1}$ | 3 % |

A simplified mechanism of the subsequent degradation of 4-hydroxynorpinonaldehyde is shown in S4. An overview of added reactions is shown in Tab. S4. Reaction rates are base on Vereecken and Peeters (2009); Vereecken and Nozière (2020). Only the main reaction branches ($\geq 5\%$) were investigated. The mechanism was constructed according to Jenkin et al. (1997). For all $RO_2 + NO$ reactions the standard reaction rate from MCM (KRO2NO) and an organic nitrate yield of 23 % was used. $RO_2 + HO_2$ reactions were included as described for the modified mechanism based on Fantechi et al. (2002). The photolysis frequency of pinononaldehyde was used for the photolysis of formed hydroperoxides (ROOH).

H-abstraction by OH mainly occurs at the aldehyde group forming the peroxy radical C1. After a rapid $CO_2$ elimination, C1 forms C2 and C3 in equal amounts. C2 can undergo an 1,5 H-shift to form a stable hydroperoxy compound (C5) and $HO_2$. Alternatively, C2 can form the alkoxy radical C4 after reaction with NO. Similarly, C3 forms the alkoxy radical C12. Ring-opening of the 4-membered ring in both C4 and C12 leads to the formation of a peroxy radical C6. Subsequently, the main fraction (approximately 90 %) rearranges after an 1,6 H-shift to C9. C9 either undergoes an 1,6 H-shift forming C10 or forms an alkoxy radical that further decomposes to a stable product and $HO_2$.

A sensitivity run (S3) using the degradation scheme of 4-hydroxynorpinonaldehyde was performed and results can be seen in Fig. S5. The modifications have only a small effect on $HO_2$ and OH concentrations. In the second half of the experiment the degradation of pinonaldehyde oxidation products becomes more relevant and additional $HO_2$ is formed by the 4-hydroxynorpinonaldehyde degradation scheme. However, the effect on the $HO_2$ concentration is small and $HO_2$ concentrations are increased by up to 10 % compared to FAN_a.

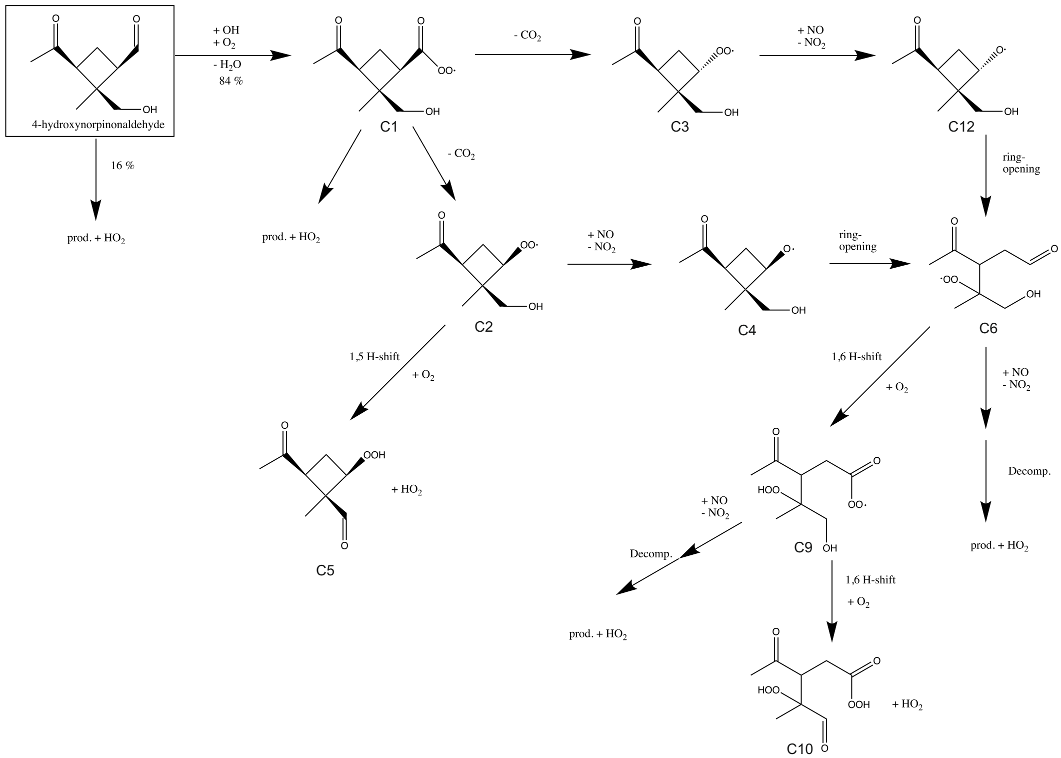

**Figure S4.** Simplified mechanism of the subsequent degradation of 4-hydroxynorpinonaldehyde. The mechanism is deduced from SAR. For details see text. $RO_2 + HO_2$ reactions and $RO_2 + NO$ reactions that form nitrates are not shown.

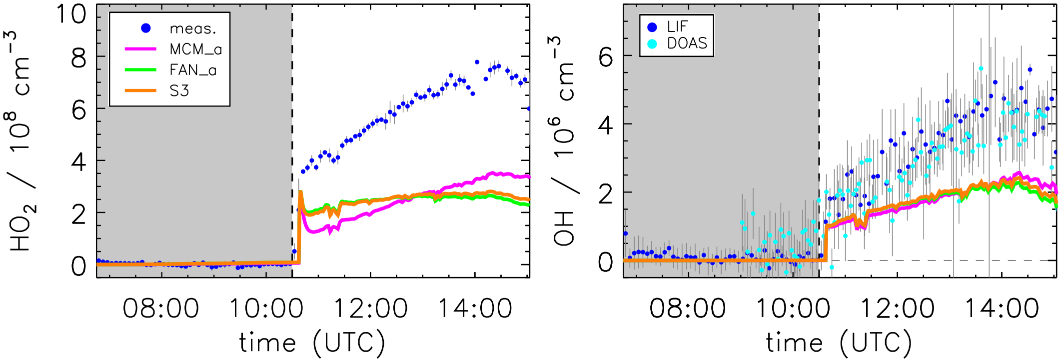

**Figure S5.** Model sensitivity study of the impact of a 4-hydroxynorpinonaldehyde degradation mechanism (S3) compared to the model base case (MCM_a) and the case using the mechanism by Fantechi et al. (2002) (FAN_a). Grey shaded areas indicate times when the chamber roof was closed.

**Table S4.** Extended mechanism for the further degradation of 4-hydroxynorpinonaldehyde used for sensitivity test S3. For details see text. All nitrate species are lumped as one species RNO3.

| reaction | reaction rate constant |
|---|---|
| NORPINALOH + OH → C1 | $1.69 \times 10^{-11}\,\mathrm{cm^3\,s^{-1}}$ [a] |
| NORPINALOH + OH → D1 + $HO_2$ | $3.27 \times 10^{-12}\,\mathrm{cm^3\,s^{-1}}$ [a] |
| NORPINALOH + OH → F1 + $HO_2$ | $5.43 \times 10^{-13}\,\mathrm{cm^3\,s^{-1}}$ [a] |
| NORPINALOH + OH → G1 + $HO_2$ | $2.62 \times 10^{-13}\,\mathrm{cm^3\,s^{-1}}$ [a] |
| NORPINALOH + OH → H1 + $HO_2$ | $5.43 \times 10^{-13}\,\mathrm{cm^3\,s^{-1}}$ [a] |
| NORPINALOH + h$\nu$ → C2 + $HO_2$ | $j_{\mathrm{PINAL}}$ |
| C1 → C2 + $CO_2$ | KDEC[b] |
| C1 → C3 + $CO_2$ | KDEC[b] |
| C1 → prod. + $HO_2$ | $9.16 \times 10^{-2}\,\mathrm{s^{-1}}$ |
| C1 + NO → C1O + $NO_2$ | 0.77*KRO2NO[c] |
| C1 + NO → RNO3 | 0.23*KRO2NO[c] |
| C1 + $HO_2$ → C1OOH | KRO2HO2[d] |
| C1OOH + OH → C1 | $1.3 \times 10^{-11}\,\mathrm{cm^3\,s^{-1}}$ |
| C1OOH + h$\nu$ → C1O + OH | $j_{\mathrm{PINAL}}$ |
| C1O→ prod. + $HO_2$ | KDEC[b] |
| C2 + NO → C4 + $NO_2$ | 0.77*KRO2NO[c] |
| C2 + NO → RNO3 | 0.23*KRO2NO[c] |
| C2 → C5 + $HO_2$ | $1.3 \times 10^{-2}\,\mathrm{s^{-1}}$ |
| C2 + $HO_2$ → C2OOH | KRO2HO2[d] |
| C2OOH + OH → C2 | $1.3 \times 10^{-11}\,\mathrm{cm^3\,s^{-1}}$ |
| C2OOH + h$\nu$ → C4 + OH | $j_{\mathrm{PINAL}}$ |
| C4 → C6 | KDEC[b] |
| C6 → C9 | $2.8 \times 10^{-1}\,\mathrm{s^{-1}}$ |
| C6 + NO → C7 + $NO_2$ | 0.77*KRO2NO[c] |
| C6 + NO → RNO3 | 0.23*KRO2NO[c] |
| C6 + $HO_2$ → C6OOH | KRO2HO2[d] |
| C6OOH + OH → C6 | $1.3 \times 10^{-11}\,\mathrm{cm^3\,s^{-1}}$ |
| C6OOH + h$\nu$ → C7 + OH | $j_{\mathrm{PINAL}}$ |
| C7 → C8 + ACETOL | KDEC[b] |
| C8 → prod. + $HO_2$ | KDEC[b] |
| C9 → C10 + $HO_2$ | $6.6 \times 10^{-4}\,\mathrm{s^{-1}}$ |
| C9 + NO → C11 + $NO_2$ | 0.77*KRO2NO[c] |
| C9 + NO → RNO3 | 0.23*KRO2NO[c] |
| C9 + $HO_2$ → C9OOH | KRO2HO2[d] |
| C9OOH + OH → C9 | $1.3 \times 10^{-11}\,\mathrm{cm^3\,s^{-1}}$ |
| C9OOH + h$\nu$ → C11 + OH | $j_{\mathrm{PINAL}}$ |
| C11 → C13 + $HO_2$ | KDEC[b] |
| C3 + NO → C12 + $NO_2$ | 0.77*KRO2NO[c] |
| C3 + NO → RNO3 | 0.23*KRO2NO[c] |
| C3 + $HO_2$ → C3OOH | KRO2HO2[d] |
| C3OOH + OH → C3 | $1.3 \times 10^{-11}\,\mathrm{cm^3\,s^{-1}}$ |
| C3OOH + h$\nu$ → C12 + OH | $j_{\mathrm{PINAL}}$ |
| C12 → C6 + $HO_2$ | KDEC[b] |

[a] value from Kwok and Atkinson (1995)
[b] value from MCM: KDEC= $1.0 \times 10^{6}\,\mathrm{s^{-1}}$ (MCM, 2017)
[c] value from MCM: KRO2NO= $2.7 \times 10^{-12}\,\exp(360\mathrm{K/T})\,\mathrm{cm^3 s^{-1}}$ (MCM, 2017)
[d] value from MCM: KRO2HO2= $2.91 \times 10^{-13}\,\exp(1300\mathrm{K/T})\,\mathrm{cm^3 s^{-1}}$ (MCM, 2017)

## Sensitivity test of additional acetone and HCHO formation by pathways II, III, and IV

In a sensitivity study it was tested if the pathways II, III, and IV that do not form 4-hydroxynorpinonaldehyde have the potential to explain the missing acetone and formaldehyde formation in the OH oxidation experiment. In a sensitivity test the first reaction step of the pathways II, III, and IV form one molecule of acetone and HCHO each. Results are shown in Fig. S6. The additional acetone and HCHO sources can reproduce observations in the first half of the experiment within the measurement uncertainty when contributions from OH reactions of product species are small. In later stages of the experiment, acetone and formaldehyde concentrations are underestimated by the sensitivity model run. Additional acetone and HCHO formation from further degradation of oxidation products not included in the MCM could explain the model-measurement discrepancy. See the response to comment 4 for more information of potential products of the degradation of 4-hydroxinorpinonaldehyde.

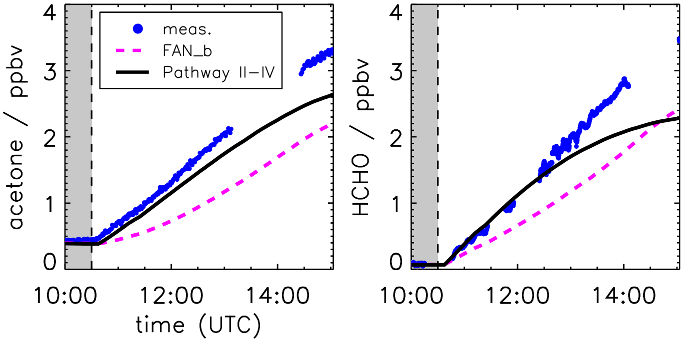

**Figure S6.** Measured and modeled formaldehyde and acetone mixing ratios for the experiment without OH scavenger. All model runs were done with measured photolysis frequencies for pinonaldehyde and with $HO_2$ constrained to measurements. Model runs were done using modifications described in Fantechi et al. (2002). For the model run shown in black an additional HCHO and acetone formation in pathways II, III, and IV is assumed.

## References

Fantechi, G., Vereecken, L., and Peeters, J.: The OH-initiated atmospheric oxidation of pinonaldehyde: Detailed theoretical study and mechanism construction, Phys. Chem. Chem. Phys., 4, 5795–5805, https://doi.org/10.1039/B205901K, 2002.

Jenkin, M. E., Saunders, S. M., and Pilling, M. J.: The tropospheric degradation of volatile organic compounds: A protocol for mechanism development, Atmos. Environ., 31, 81–104, https://doi.org/10.1016/S1352-2310(96)00105-7, 1997.

Kwok, E. S. C. and Atkinson, R.: Estimation of hydroxyl radical reaction rate constants for gas-phase organic compounds using a structure-reactivity relationship: An update, Atmos. Environ., 29, 1685–1695, https://doi.org/10.1016/1352-2310(95)00069-B, 1995.

MCM: Master Chemical Mechanism, http://mcm.leeds.ac.uk/MCM/, last access: 04 March 2020, 2017.

Vereecken, L. and Nozière, B.: H migration in peroxy radicals under atmospheric conditions, Atmos. Chem. Phys., 20, 7429–7458, https://doi.org/10.5194/acp-20-7429-2020, 2020.

Vereecken, L. and Peeters, J.: Decomposition of substituted alkoxy radicals-part I: a generalized structure-activity relationship for reaction barrier heights, Phys. Chem. Chem. Phys., 11, 9062–9074, https://doi.org/10.1039/B909712K, 2009.